Proteomic analysis and protein carbonylation profile in trained and untrained rat muscle

JOURNAL OF PROTEOMICS 75 (2012) 978–992

Available online at www.sciencedirect.com

SciVerse ScienceDirect

www.elsevier.com/locate/jprot

Proteomic analysis and protein carbonylation profile in trained and untrained rat muscles

Francesca Magherini[a,*], *Provvidenza Maria Abruzzo*[b], *Michele Puglia*[c], *Luca Bini*[c], *Tania Gamberi*[a], *Fabio Esposito*[d], *Arsenio Veicsteinas*[d], *Marina Marini*[b], *Claudia Fiorillo*[a], *Massimo Gulisano*[e], *Alessandra Modesti*[a]

[a]*Department of Biochemistry, University of Florence, Florence, Italy*
[b]*Department of Histology, Embryology, and Applied Biology, University of Bologna, Bologna, Italy*
[c]*Laboratory of Functional Proteomics, Molecular Biology Department, University of Siena, Siena, Italy*
[d]*Department of Sport Sciences, Nutrition, and Health, University of Milan, Milan, Italy*
[e]*Department of Anatomy, Histology and Legal Medicine, University of Florence, Florence, Italy*

ARTICLE INFO

Article history:
Received 25 July 2011
Accepted 21 October 2011
Available online 29 October 2011

Keywords:
Exercise training
Muscle
Oxidative stress
Carbonylation
Two dimensional gel electrophoresis
Oxyblots

ABSTRACT

Understanding the relationship between physical exercise, reactive oxygen species and skeletal muscle modification is important in order to better identify the benefits or the damages that appropriate or inappropriate exercise can induce. Unbalanced ROS levels can lead to oxidation of cellular macromolecules and a major class of protein oxidative modification is carbonylation. The aim of this investigation was to study muscle protein expression and carbonylation patterns in trained and untrained animal models. We analyzed two muscles characterized by different metabolisms: tibialis anterior and soleus. Whilst tibialis anterior is mostly composed of fast-twitch fibers, the soleus muscle is mostly composed of slow-twitch fibers. By a proteomic approach we identified 15 protein spots whose expression is influenced by training. Among them in tibialis anterior we observed a down-regulation of several glycolitic enzymes. Concerning carbonylation, we observed the existence of a high basal level of protein carbonylation. Although this level shows some variation among individual animals, several proteins (mostly involved in energy metabolism, muscle contraction, and stress response) appear carbonylated in all animals and in both types of skeletal muscle. Moreover we identified 13 spots whose carbonylation increases after training.

1. Introduction

How physical exercise affects muscles depends on both mode, intensity and duration of training and specific characteristics of the skeletal muscle in question. In skeletal muscles, reactive oxygen (ROS) and nitrogen species (RNS) are normally synthesized at low levels and are required for normal force production [1–3]. Physical activity and its relative increase in oxygen consumption can lead to a temporary unbalance between production and disposal of ROS. To better understand the benefits or the damages that an appropriate or inappropriate exercise can induce, it is necessary to study the relationship between physical exercise, ROS and skeletal muscle modification. In fact, during intense activity, the high rate of O_2

* *Corresponding author at:* Department of Biochemistry, Università degli Studi di Firenze, Viale Morgagni 50, 50134 Firenze, Italy. Tel.: +39 0554598331; fax: +39 0554598905.
E-mail address: francesca.magherini@unifi.it (F. Magherini).

1874-3919/$ – see front matter © 2011 Elsevier B.V. All rights reserved.
doi:10.1016/j.jprot.2011.10.017

consumption can cause incomplete oxygen reduction, and lead to the generation of ROS. High levels of ROS have been associated to cellular dysfunction due to DNA, protein and lipid oxidation. Although many early studies have considered exercise-induced ROS production as a potential detriment to physiological functions, recent studies are investigating an alternative role for ROS in exercise-induced muscle adaptation [4]. It is important to remember that ROS production may be quantitatively limited or counteracted by anti-oxidants, to prevent the establishment of an oxidative state. Among the various anti-oxidant systems, protein side-chain functional groups are estimated to capture 50–75% of all highly reactive oxygen species [5]. ROS may cause reversible and/or irreversible modifications on protein targets. Cysteine residues, for example, exist not only in fully reduced form (−SH) but also in different oxidation states that are partly reversible and can change relatively to the cell's redox state [6–8]. The introduction of carbonyl groups into proteins is another oxidative, non-enzymatic modification that occurs either as a result of direct attack by ROS or indirectly, through peroxidation of lipids that further attack protein acid residues [9]. Protein carbonylation can result in the unfolding or alteration of protein structure and function [10]. The evaluation of carbonylation groups is thought to be a good estimate of the extent of oxidative damage associated with aging, disease, toxic processes and physical exercise [11–14]. In the past, the carbonylation process has been considered an irreversible process, following which damaged proteins are send to proteasome for degradation. Recently, however, Wong et al. [15,16] discovered that not all carbonylated proteins are degraded by the proteasome and propose that protein carbonylation and decarbonylation are included in a signal transduction mechanism.

A significant increase in muscle protein carbonylation following prolonged inactivity [17,18], during aging [19,20], and after physical exercise [21,22] has been demonstrated. The relationship between oxidative stress and training has also been evaluated by measuring plasma protein carbonylation [23]. These studies assayed total carbonyl content without identifying specific oxidation protein targets. In a previous paper we identified, by proteomic analysis, plasma proteins that undergo carbonylation in response to physical exercise [24]. We found proteins that underwent carbonylation: 1) only after physical exercise, 2) independently of exercise, and 3) only in resting condition. Among the first group of carbonylated proteins, we reported Haptoglobin, a plasma glycoprotein whose main function is to protect Hemoglobin from oxidative damage and which is reported to be a risk factor in several oxidative stress-related diseases. Among the third group proteins, we found Serotransferrin and Fibrinogen which are thought to be the most susceptible to oxidation and show a reduced carbonylation level after physical exercise, thus suggesting a possible beneficial effect of the latter. The fact that a large number of carbonylated proteins was found to be carbonylated in resting condition means that carbonylation is a normal metabolic process [25]. It is yet early days for the application of proteomics in the investigation of the impact exercise has on muscle protein expression and modification and only few studies on this subject have been published [26–30].

In this study we investigate how aerobic training influences protein expression and formation of protein carbonyl adducts in two types of skeletal muscle characterized by different energetic metabolisms: tibialis anterior and soleus. The tibialis anterior is mostly composed of fast-twitch fibers that have a high potential in ATP production by anaerobic pathway. The soleus, on the other hand, is mostly composed of slow-twitch fibers which are characterized by a high aerobic metabolism. In order to analyze the level of muscle oxidative stress following controlled training conditions, we used experimental animal models. Rats were assigned to either a sedentary or an exercise group. Exercise group rats were subjected to a 10-week aerobic training in order to reach ~80% VO_2max which corresponds to the consumption level reached by well-trained non-professional human athletes. The carbonylated protein pattern was studied by two-dimensional gel electrophoresis (2-DE) followed by Western blot (WB) with anti-dinitrophenyl hydrazone (DNP) antibodies. Studying two different muscle types, also enabled us to investigate whether an increase in oxidative stress is muscle specific. The aims of this study were the analysis of protein expression variation and oxidation induced by training, with special regard to: (a) explore whether different muscle types show an increase in oxidative stress after training; (b) identify the nature of oxidatively modified proteins (protein carbonylation indices); and (c) evaluate the possibility of a fiber-type specificity in protein oxidation.

2. Materials and methods

2.1. *Animal models and controlled exercise training*

In our experiment, we used male albino Sprague–Dawley rats, aged two months at entry. Rats (four control rats and four trained rats) were housed in individual cages and fed standard diet without limitations. Room temperature was kept at 21 ± 2 °C and 12 h of light were automatically alternated with 12 h of dark. The University Committee for the Use of Laboratory Animals approved animal handling, training protocol and mode of sacrifice. The investigation conformed to the American Physiological Society guidelines for exercising rodents on treadmills (American Physiological Society, 2006, http://www.the-aps.org/pa/action/exercise/book.pdf) and to the Guide for Care and Use of Laboratory Animals published by the National Institutes of Health [31]. After one week of acclimatization, rats were progressively trained in order to reach ~80% of VO_2max in 4 weeks. This workload was maintained for 6 weeks. At the end of this protocol, speed was 25 m/min at 10% slope. Training consisted in one hour morning exercise 3 times a week, using a 6-lane rodent treadmill at 10% slope. We used a control group of untrained rats which were placed on a non-moving treadmill during training sessions. Rats were anesthetized 1 h after the last training session with i.p. sodium thiopental (50 mg/kg) and weighed. They were then sacrificed by removal of the heart, which was used for other analyses. Hind limbs were opened and tibialis anterior and soleus muscles were isolated. After trimming excess water and connective tissue, the muscles were frozen in liquid nitrogen and stored at −80 °C until use for biochemical evaluations.

2.2. Muscle processing and 2-DE

Frozen muscles were ground in dry ice in a cooled mortar, suspended in lysis buffer (50 mM Tris–HCl pH 7.0, 150 mM NaCl, 2 mM EGTA, 100 mM NaF, 1% (v/v) NP-40, 0.5% (w/v) deoxycholate, 0.1% (w/v) SDS containing a cocktail of protease inhibitors (Sigma) and solubilised by sonication on ice. After centrifugation proteins were precipitated following a chloroform/methanol protocol [32] and resuspended in 8 M urea, 4% (w/v) CHAPS, 65 mM DTT. Eighteen centimeter IPG-strips pH 3–10 NL were rehydrated overnight at room temperature in 350 μL of rehydration buffer containing 8 M urea, 2% (w/v) CHAPS, 0.5% DTT 0.5% (w/v) IPG buffer, having the same pH range as the Immobiline DryStrips, and a trace of Bromophenol blue. Rehydrated strips were rinsed in double-distilled water to remove urea crystals. Samples (60 μg and 750 μg for analytical and preparative gels respectively) were cup-loaded near the anode of the IPG strips using Ettan IPGphor cuploading manifold (GE Healthcare) according to the manufacturer's protocol. The strips were focused at 20 °C according to the following electrical conditions: 200 V for 1 h, from 300 V to 3500 V in 30 min, 3500 V for 3 h, from 3500 V to 8000 V in 30 min, and 8000 V until a total of 80,000 V/h was reached. After focusing, analytical and preparative IPG strips were equilibrated for 10 min in 6 M urea, 30% (v/v) glycerol, 2% (w/v) SDS, 2% (w/v) DTT in 0.05 M Tris–HCl buffer, pH 6.8, and subsequently for 10 min in the same buffer solution where DTT was substituted with 2.5% (w/v) iodoacetamide. The second dimension was carried out on 9–16% polyacrylamide linear gradient gels (18 cm × 20 cm × 1.5 mm) at 10 °C and 40 mA/gel constant current until the dye front reached the bottom of the gel. Analytical gels were stained with ammoniacal silver nitrate as previously described [33]; MS-preparative gels were stained with colloidal Coomassie [34].

2.3. Derivatization and immunodetection of protein carbonyls (oxyblot)

After first dimension electrophoresis, protein carbonyls were derivatized to DNP by incubating IPG strips in 10 mM DNPH dissolved in 2 N HCl, for 20 min at room temperature. After washing the strips with 6 M Urea, 20% (v/v) Glycerol, 1% (w/v) SDS, 150 mM Tris–HCl, pH 6.8, the strips were reduced, alkylated and run on 9–16% polyacrylamide linear gradient gels (18 cm × 20 cm × 1.5 mm). After running, gels were blotted overnight on Polyvinylidene Fluoride (PVDF) membrane. The PVDF membranes were incubated for 3 h at 4 °C with the primary antibody solution consisting of a 1:10,000 dilution of the anti-DNP IgG antibody (Sigma) in Phosphate-buffered saline (PBS) containing 5.0% non-fat dry milk. The blots were then washed with PBS, 0.1% (v/v) Tween and incubated with the goat anti-rabbit IgG/HRP conjugate (1:3000 dilution in PBS/Milk) for 1 h at room temperature. An enhanced chemiluminescence kit (Immobilon Western Chemiluminescent AP substrate, Millipore) was used for detection. The detection of protein carbonyl groups on PVDF membrane after 1-DE, was performed according to Dalle Donne et al. [35]. Briefly the membrane was incubated for 5 min with 0.1 mg/ml of DNPH dissolved in 2 N HCl and then washed 3 times in 2 N HCl and 7 times in 100% methanol (5 min each). The immunodetection of DNP-derivate was performed as described for PVDF membrane from 2-DE gels.

2.4. Image acquisition and analysis

Gel and oxyblot images were acquired using an Epson expression 1680 PRO scanner and saved as TIFF files. Computer-aided 2D image analysis was carried out using ImageMaster 2D Platinum software version 6.0 (GE Healthcare). Relative spot volume (% V=V single spot/V total spots, where V is the integration of the optical density over the spot area) was used during analysis in order to reduce experimental error. The intensity of carbonylated spots on Oxyblots was normalized vs their respective spots visualized on silver stained gels.

2.5. Mass spectrometry (MS) protein identification

Protein identification was carried out by peptide mass fingerprinting (PMF) on Ettan MALDI-TOF Pro mass spectometer (GE Healthcare) as previously described [36]. After visualization by colloidal Coomassie staining protocol, spots were mechanically excised, destained in 2.5 mM ammonium bicarbonate and 50% (v/v) acetonitrile and finally dehydrated in acetonitrile. They were then rehydratated in trypsin solution and in-gel protein digestion was performed by overnight incubation at 37 °C. Each protein digest (0.75 μL) was spotted onto the MALDI target and allowed to air dry. Then 0.75 μL of matrix solution (saturated solution of α-cyano-4-hydroxycinnamic acid in 50% (v/v) acetonitrile and 0.5% (v/v) TFA) was applied to the sample which was then dried again. Mass spectra were acquired automatically using the Ettan MALDI Evaluation software (GE Healthcare). Spectra were internally calibrated using the autoproteolysis peptides of trypsin (842.51 and 2211.10 Da). Protein identification by Peptide Mass Fingerprints search was performed using MASCOT version 2.2 as the search engine (Matrix Science, London, UK, http://www.matrixscience.com) through the Swiss-Prot/UniprotKB database. Taxonomy was limited to *Rattus norvegicus*, a mass tolerance of 100 ppm was allowed and the number of accepted missed cleavage sites was set to one. Alkylation of cysteine by carbamidomethylation was considered a fixed modification, while oxidation of methionine was considered as a possible modification. The criteria used to accept identifications included the extent of sequence coverage (at least 10%), the number of matched peptides (at least 5) and a probabilistic score at $p<0.05$.

2.6. Western blot and immunoprecipitation analysis of proteomics candidates

For 1-DE 20 μg of protein extracts were separated by 12% SDS-PAGE and transferred onto a PVDF membrane (Millipore). The relative amount of enolase protein was assessed by Western blot with appropriate antibodies (Santa Cruz Biotechnology). For quantification, the blots were stained with Coomassie brilliant blue R-250 and subjected to densitometric analysis performed using Quantity One Software (Bio-Rad). Statistical analysis of the data was performed by Student's *t*-test; p-values 0.05 were considered statistically significant. The intensity of the immunostained bands were normalized with the total protein intensities

measured by Coomassie brilliant blue R-250 from the same blot. For the immunoprecipitation 500 μg of total proteins were incubated with the specified antibodies (anti-aldolase A, anti-actin, anti-enolase, all from Santa Cruz Biotechnology) in RIPA buffer and the immunocomplexes were collected on protein A-Sepharose (Sigma), separated by gel electrophoresis, and transferred to PVDF.

2.7. Catalase activity

Catalase activity was measured in tibialis anterior and soleus skeletal muscle by the colorimetric assay described by Goth [37]. Frozen skeletal muscles from control and trained rats were crushed to powder using a ceramic mortar and pestle. The powder was homogenized in a lysis buffer containing 0.1 M sodium phosphate buffer, pH 7.0 and 3% Protease Inhibitor Cocktail (Sigma-Aldrich, St. Louis, MO). The homogenate was clarified by centrifugation at 4 °C at 10,000×*g* for 10 min to remove cell debris. The supernatant was incubated with H_2O_2 (65 μmol/ml in a 6.0 mM sodium–potassium phosphate buffer, pH 7.4) at 37 °C for 60 s; the enzymatic reaction was stopped by the addition of 32.4 mM ammonium molybdate (Sigma-Aldrich, St. Louis, MO). The intensity of the yellow complex formed by molybdate and the remaining H_2O_2 were measured at 405 nm using a 96-well plate reader (Victor2 Multilabel Counter, Perkin-Elmer, Waltham, MA). Catalase from bovine liver (Sigma-Aldrich, St. Louis, MO) was used as a standard for the estimation of Catalase activity, expressed in units per milligram of protein.

2.8. SOD activity

SOD activity was determined in tibialis anterior and soleus skeletal muscles by a competitive colorimetric inhibition assay as previously described [38,39]. This method is based on the ability of superoxide ions, generated by xanthine and xanthine oxidase, (Sigma-Aldrich) to reduce WST-1 (2-(4-iodophenyl)-3-(4-nitrophenyl)-5-(2,4-disulfophenyl)-2H-tetrazolium, monosodium salt (Dojindo Laboratories Co., Kumamoto, Japan) to a water-soluble formazan dye. SOD activity reduces superoxide concentration and inhibits formazan formation. Tibialis anterior and soleus skeletal muscles were crushed to powder using a ceramic mortar and pestle. The powder was homogenized in a lysis buffer containing 10 mM Tris, 1 mM EDTA, 0.1% (v/v) Triton X-100 and 3% Protease Inhibitor Cocktail (Sigma-Aldrich, St. Louis, MO). The homogenate was clarified by centrifugation at 4 °C at 10,000×*g* for 10 min to remove cell debris. The supernatant was incubated with a reaction mixture containing 500 μM WST–1.50 μM xanthine and xanthine oxidase (29 mU/mL) in 50 mM CHES (2-N-(Cyclohexylamino) ethanesulphonic acid, Sigma-Aldrich, St. Louis, MO), pH 8.0. Mn-SOD (SOD-2) activity was evaluated adding 1 mM KCN to inhibit cytosolic Cu,Zn-SOD (SOD-1). Formazan formation was measured at 450 nm using a 96-well plate reader (Victor2

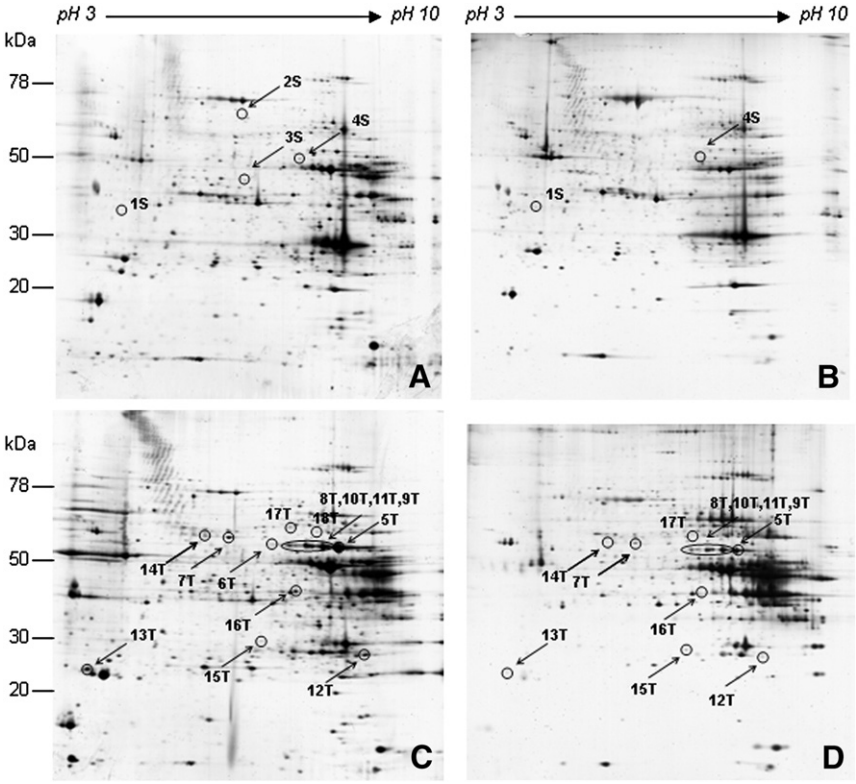

Fig. 1 – Representative 2-DE images of muscles protein extracts run on NL pH 3–10 IPG strip and in 9–16% polyacrylamide linear gradient. Soleus untrained (A), soleus trained (B), and tibialis anterior untrained (C), tibialis anterior trained (D). Circles and numbers indicate spots differentially expressed after training. Arrows indicate the spots identified by MS.

Multilabel Counter, Perkin-Elmer, Waltham, MA). SOD activity, expressed in units per milligram of protein, was determined using a SOD reference curve.

2.9. TBARS measurement

As a lipid peroxidation marker, we measured thiobarbituric acid reactive substances (TBARS) according to the method described by Ohkawa et al. [40]. Malondialdehyde (MDA), measures were expressed in nanomoles per mg of proteins.

2.10. Statistical analyses

All data are presented as mean ± standard deviation. Differences between sedentary and trained rats were determined using Student's two tailed independent *t*-test. *p* values of ≤0.05% were considered significant.

3. Results

3.1. Differential protein expression in trained versus untrained soleus and tibialis anterior muscles

In order to evaluate the impact of training on the proteins of two muscle types, we studied the differences between protein expression profiles of untrained and trained muscles by 2-DE. The proteins were separated and resolved in all areas of the gels and an average of 900 spots were detected on silver stained gels using ImageMaster 2D Platinum software version 6.0. Each protein sample was run in triplicate to obtain statistically significant results. Fig. 1 reports representative gel images of soleus and tibialis anterior before (A and C respectively) and after (B and D respectively) training. The parameters used to assay the significance of expression variation were: a fold change of 1.8 in relative spot volume (%V = V single spot/V total spots, where V is the integration of the optical density over the spot area) and a *t*-test statistical probability less than 0.05 ($p<0.05$). The spots that satisfied these criteria are circled in Fig. 1. Of these, 14 spots (spots 5T–18T) were detected in the tibialis anterior muscle (C, D) whereas in the soleus muscle (A, B) only 4 spots (spots 1S–4S) varied after training. Table 1 shows the quantitative data and statistical analyses of protein spots whose intensity levels significantly differed between trained and untrained rats. In trained tibialis anterior 12 spots (spots 5T, 7T, 8T, 9T, 10T, 11T, 12T, 13T, 14T, 15T, 16T and 17T) showed a down-regulation in comparison to the untrained muscle and two spots (spots 6T and 18T) were detected only in the untrained condition. In soleus muscle one spot (spot 3S) showed an increase and one spot (spot 4S) a decrease in expression level when trained. In this muscle two protein spots (spots S1 and S2) were detected exclusively after training. %V of 8 protein spots (spots 5T, 7T, 8T, 9T, 10T, 14T, 15T and 17T) changed significantly with a confidence level above 99% ($p<0.01$) whilst the %V of other 6 protein spots (spots 11T, 12T, 13T, 16T, 3S and 4S) changed

Table 1 – Quantitative data and statistical analyses of protein spots whose %V differed significantly between untrained and trained rats. S indicates spots found in soleus muscle and T in tibialis anterior muscle.

Spot detected in both untrained and trained muscles				
Spot no. [a]	%V mean ± SD [b] untrained muscles	%V mean ± SD [b] trained muscles	Fold change [c] (%V untrained/%V trained)	*p*-value [d]
3S	0.023 ± 0.029	0.063 ± 0.005	−2.7	0.017
4S	0.039 ± 0.024	0.012 ± 0.003	3.2	0.04
5T	1.834 ± 0.059	0.937 ± 0.067	1.9	0.0001
7T	0.16 ± 0.019	0.059 ± 0.0126	2.7	0.0018
8T	0.112 ± 0.012	0.0468 ± 0.009	2.4	0.0029
9T	1.25 ± 0.1698	0.435 ± 0.119	2.9	0.0035
10T	0.436 ± 0.102	0.124 ± 0.0259	3.5	0.0072
11T	0.213 ± 0.02496	0.114 ± 0.021	1.8	0.0177
12T	0.23 ± 0.043	0.0931 ± 0.03	2.5	0.0306
13T	0.291 ± 0.018	0.125 ± 0.052	2.4	0.0364
14T	0.12 ± 0.068	0.023 ± 0.013	5.2	0.008
15T	0.1 ± 0.02	0.0467 ± 0.027	2.1	0.009
16T	0.158 ± 0.045	0.0808 ± 0.048	1.95	0.037
17T	0.026 ± 0.007	0.0108 ± 0.005	2.4	0.004

Spots detected only in untrained or trained muscles		
Spot no. [a]	%V mean ± SD [b] untrained muscle	%V mean ± SD [b] trained
1S	Not detected	0.01 ± 0.003
2S	Not detected	0.017 ± 0.006
6T	0.041 ± 0.015	Not detected
18T	0.016 ± 0.008	Not detected

[a] Spot numbers match those reported in the representative 2-DE images shown in Fig. 1.
[b] Values represent mean ± standard deviation of individually computed %V of indicated spot (V = integration of OD over the spot area; %V = V single spot/V total spots).
[c] Fold change (untrained vs. trained) was calculated as follow: $\%V_{untrained}/\%V_{trained}$.
[d] Student's *t*-test was performed to determine if the relative change was statistically significant ($p<0.05$).

significantly with a confidence level between 99% and 96% ($0.01 \leq p \leq 0.04$).

3.2. Protein identification by mass spectrometry

Thirteen differentially expressed spots (spots 3S, 4S, 7T, 14T, 5T, 8T, 9T, 10T, 11T, 12T, 15T, 13T and 16T) as well as two spots (spots S2 and T6) which were detected exclusively in one condition were excised from preparative Coomassie-stained 2-DE gels obtained from 2 pools: one from trained and untrained soleus muscles and the other from trained and untrained tibialis anterior muscles (Figs. 1s and 2s). These spots were in-gel digested with trypsin, and subsequently analyzed by mass spectrometry. All identified proteins are described in Table 2 and are indicated by arrows and numbers in Fig. 1. The sequence coverage of the proteins identified ranges between 22 and 47% depending on protein size and amount. In trained tibialis anterior muscle two spots corresponding to Alpha-enolase (spots 7T and 14T) and five of Beta-enolase (spots 5T, 8T, 9T, 10T and 11T), are down-regulated. Both proteins are glycolitic enzymes but they participate in many other physiological and pathological processes; such as growth control, hypoxia tolerance and striated muscle development and regeneration [41,42]. Another glycolitic enzyme which is down-regulated in trained rats is Triose-phosphate isomerase (spot 15T) that converts D-glyceraldehyde 3-phosphate in glycerone phosphate and vice versa. The fact that important glycolitic enzymes show a reduced expression after training probably indicates a partial switch to an aerobic metabolism. Also down-regulated after training are ES1 protein homolog (spot 12T), Lactoylglutathione lyase (spot 13T) and Creatine kinase M-type (spot 16T). ES1 protein belongs to the ES1 family characterized by an N-terminal presequence which directs them to mitochondria. Lactoylglutathione lyase (spot 13T) catalyzes the conversion of hemimercaptal, formed from methylglyoxal and glutathione, to S-lactoylglutathione. Methylglyoxal is a toxic by-product of glycolysis and other metabolic pathways. In mammalian cells the principal route for detoxification of this reactive metabolite is via the glutathione-dependent D-lactate forming glyoxalase pathway which involves lactoylglutathione lyase. Creatine kinase (spot 16T) reversibly catalyzes the transfer of phosphate between ATP and various phosphogens (e.g. creatine phosphate). It has a role in energy transduction in tissues with large, fluctuating energy demands, such as that of skeletal muscles. In soleus muscles we identified two proteins whose expression levels are reduced after training: mitochondrial NADH dehydrogenase 1 alpha subcomplex (spot 3S) and mitochondrial Elongation factor Tu (spot 4S). Mitochondrial NADH dehydrogenase 1 alpha subcomplex is an accessory subunit of the mitochondrial membrane respiratory Complex I. This complex is activated during the transfer of electrons from NADH to the respiratory chain. The mitochondrial Elongation factor Tu (spot 4S) promotes the binding of aminoacyl-tRNA to ribosomes during protein biosynthesis. Among the proteins expressed exclusively in untrained tibialis anterior we identified an isoenzyme of Beta-enolase (spot 6T) whilst we identified exclusively in trained soleus muscle Disulfide-isomerase A3 (spot 2S), protein which catalyzes –S–S– bond rearrangement in proteins.

Table 2 – MALDI-TOF analysis of muscle proteins whose expression levels significantly differs between trained and untrained rats.

Spot no. [a]	Accession no. [b]	Protein name	MASCOT search results [c]		Score	Theoretical MW (kDa)/pI
			Matched peptides/ searched peptides	Sequence coverage		
Spots detected only in both trained and untrained muscles						
3S	Q561S0	NADH dehydrogenase [ubiquinone] 1 alpha subcomplex subunit 10, mitochondrial	10/18	43%	122	40,753/7.64
4S	P85834	Elongation factor Tu, mitochondrial	12/14	32%	163	49,890/7.23
7T	P04764	Alpha-enolase	11/17	31%	105	47,440/6.16
14T	P04764	Alpha-enolase	11/21	32%	94	47,440/6.16
5T	P15429	Beta-enolase	13/19	34%	122	47,326/7.08
8T	P15429	Beta-enolase	11/19	34%	113	47,326/7.08
9T	P15429	Beta-enolase	11/15	28%	111	47,326/7.08
10T	P15429	Beta-enolase	9/13	31%	113	47,326/7.08
11T	P15429	Beta-enolase	10/26	28%	70	47,326/7.08
12T	P56571	ES1 protein homolog, mitochondria	9/19	47%	100	28,497/9.11
15 T	P48500	Triosephosphate isomeras	8/17	41%	112	27,345/6.89
13 T	Q6P7Q4	Lactoylglutathione lyase	9/16	46%	120	20,977/5.12
16 T	P00564	Creatine kinase M-type	8/13	26%	102	43,246/6.58
Spots detected only in trained or untrained muscles						
2S	P11598	Protein disulfide-isomerase A3	11/18	22%	120	57,044/5.88
6 T	P15429	Beta-enolase	11/16	30%	108	47,326/7.08

[a] Spot numbers match those reported in the representative 2-DE images shown in Fig. 1.
[b] Accession number in Swiss-Prot/UniprotKB.
[c] MASCOT search results: number of matched peptides correspond to peptide masses matching the top hit from Ms-Fit PMF, searched peptide are also reported; sequence coverage indicates [number of identified residues/total number of amino acid residues in the protein sequence] × 100%; score corresponds to MASCOT score (MatrixScience, London, UK; http://www.matrixscience.com).

3.3. *Training induced protein carbonylation*

In order to discover variations in protein oxidation induced by training, we evaluated the protein carbonylation pattern by proteomic approach in both tibialis anterior and soleus muscles. We marked carbonylated proteins with DNPH and the DNP-derivates, after detection by specific antibody, were analyzed using 2-DE followed by Western blot (Oxyblots). Fig. 2 shows a representative image of the Oxyblots obtained from untrained soleus and tibialis anterior muscles (A and C) and trained soleus and tibialis anterior muscles (B and D). In order to exclude non-specific staining, we performed an experiment during which the incubation of IPG strips with DNPH was omitted. In this condition no DNP-derivate can be obtained. The PVDF membrane was then incubated with DNP-antibodies as described in materials and methods. The spot corresponding to the faint signal detected in the oxyblot from soleus muscle was excluded from analysis (Fig. 3s of supplementary materials). Oxyblot images were analyzed using Imagemaster 2D Platinum software and the normalization of immunoreactive spots was performed against their respectives on silver stained gels. A mean of 265±50 and 306±17 carbonylated spots was detected in soleus from untrained and trained rats respectively. In tibialis anterior muscles the mean of carbonylated spots was 191±31 for untrained rats and 202±10 for trained rats. We compared % V values of spots on Oxyblots of control muscles with those on Oxyblots obtained after training. We considered modified in carbonylation those spots whose %V in post-training Oxyblots was at least 1.8-fold higher or lower than that in untrained muscle Oxyblots. Only the reproducible differences were taken into account. From this analysis we found 13 protein spots that were differentially carbonylated between untrained and trained soleus muscles (Fig. 2, panels A and B) and 16 differentially carbonylated spots between untrained and trained tibialis anterior muscles (Fig. 2, panels C and D). These protein spots are circled in Fig. 2.

3.4. *Identification of proteins whose carbonylation is affected by training*

In order to identify significant spots, we performed preparative gels which were then colloidal Coomassie-stained (Figs. 1s and 2s). The oxyblot images were matched to the corresponding colloidal Coomassie stained 2-DE gels and the spots that corresponded to carbonylated proteins were cut and subjected to mass spectrometry analysis. The increment of protein load caused an expected loss of separative power and some carbonylated spots, detectable with silver staining, were not clearly detected in Coomassie stained gels (Fig. 2, white circles). Among the protein spots showing a modified

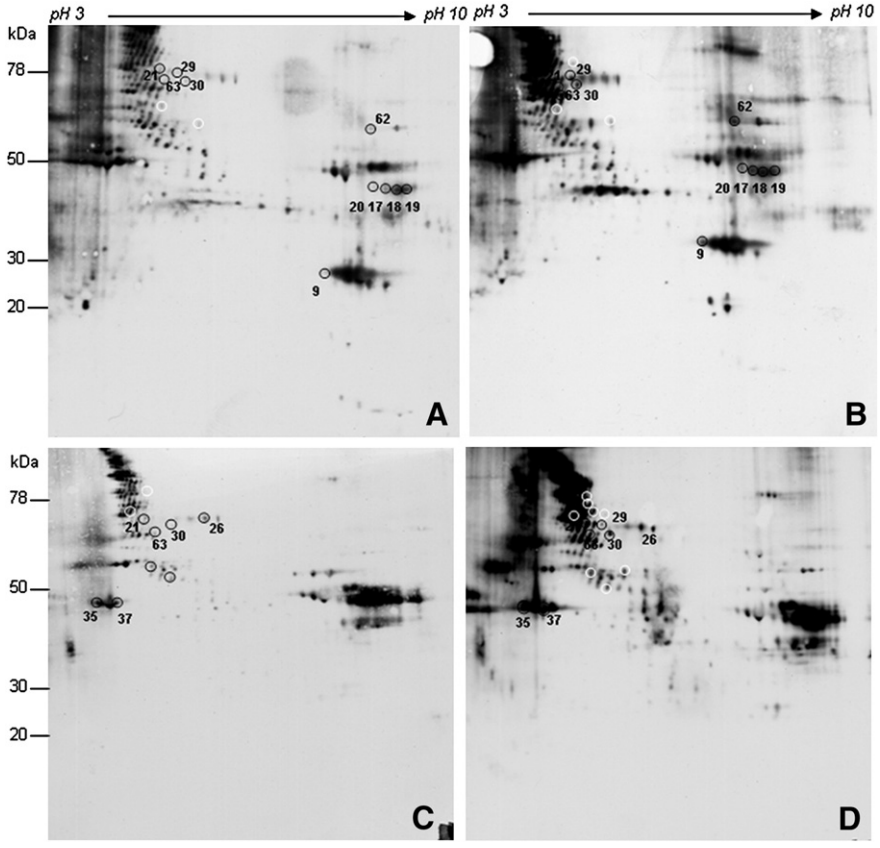

Fig. 2 – Western-blots probed with anti-DNP antibodies to detect DNPH-reactive carbonyl groups in skeletal muscle proteins. Proteins from soleus untrained (A), soleus trained (B), tibialis anterior untrained (C), and tibialis anterior trained (D) were separated by IEF and carbonylated proteins were derivatized with DNPH in the strip (18 cm, 3–10 NL). Second dimension was performed in 9–16% polyacrylamide linear gradient. Circles (black and white) indicated spots which carbonylation was affected by training. Black circles and number indicate spots identified by MS.

carbonylation level, we identified 14 spots by mass spectrometry (Table 3) which are indicated by black circles and numbers in Fig. 2. Mass data of spots reported in Table 3 can be found in Table 1s (supplementary materials). Six protein spots present an increased in carbonylation level only in soleus muscles. Among these we found two spots corresponding to Carbonic anhydrase 3 (spots 9S and 62S) and 4 spots corresponding to Fructose-bisphosphate aldolase A (spots 17S, 18S, 19S and 20S. Carbonic anhydrase 3 (CA3) is a member of a multigene family that encodes carbonic anhydrase isozymes. These carbonic anhydrases are a class of metalloenzymes that catalyze the reversible hydration of carbon dioxide and are differentially expressed in various cell types. The expression of the CA3 gene is strictly tissue specific and present at high levels in skeletal muscles and at much lower levels in cardiac and smooth muscles; Fructose-bisphosphate aldolase A is a glycolytic enzyme present in several isoforms on the 2-DE gels. These isoforms show a different carbonylation intensity after training (spot 17S shows a 2.5-fold change and spots 18S, 19S and 20S show a 4.3-fold change). This could indicate that some isoforms are more susceptible to oxidation than others, probably due to their specific structural features. Three spots corresponding to the structural protein Actin (spots 5T, 37T and 61T) present an increased carbonylation only in trained tibialis anterior muscles whereas Myosin-7 (spots 63T and 63S) carbonylation is up-regulated in both trained tibialis anterior and soleus muscles. Mitochondrial Stress-70 protein (spots 21T and 21S) and Heat shock protein 1A/1B (spots 29T and 29S) also show an increased carbonylation level after training in both muscle types. Both proteins are members of the heat shock protein 70 family and play a role in the processing of cytosolic and secretory proteins as well as in the removal of denatured or incorrectly-folded proteins. We also found an up-regulation in the post-training carbonylation level of Dihydrolipoyllysine-residue acetyltransferase component of pyruvate dehydrogenase complex (spots 30T and 30S). This protein catalyzes the conversion of pyruvate to acetyl-CoA and CO_2.

Table 3 – Identity of muscle proteins whose carbonylation is affected by training.

Spot no. [a]	Accession number [b]	Protein name	Fold change [c] (%V trained/ %V untrained)
9S	P14141	Carbonic anhydrase 3	Only in trained soleus muscle
62S	P14141	Carbonic anhydrase 3	2.5
17S	P05065	Fructose-bisphosphate aldolase A	2.5
18S	P05065	Fructose-bisphosphate aldolase A	4.3
19S	P05065	Fructose-bisphosphate aldolase A	4.3
20S	P05065	Fructose-bisphosphate aldolase A	4.3
21S	P48721	Stress-70 protein, mitochondrial	5
21T			4
29S	Q07439	Heat shock 70 kDa protein 1A/1B	4.3
29T			Only in trained muscles
30S	P08461	Dihydrolipoyllysine-residue acetyltransferase component of pyruvate dehydrogenase complex, mitochondrial	2.6
30T			30
26T	P02770	Serum albumin	−1.8
63S	P02563	Myosin-7	17
63T			8
35T	P68136	Actin, alpha skeletal muscle	1.8
37T	P68136	Actin, alpha skeletal muscle	1.9
61T	P68136	Actin, alpha skeletal muscle	2.1

[a] Spot numbers match those reported in the representative 2-DE images shown in Fig. 2.
[b] Accession number in Swiss-Prot/UniprotKB.
[c] Fold change trained vs. untrained was calculated as follow:% $V_{untrained}/\%V_{trained}$. ($p<0.05$).

3.5. *A basal level of protein carbonylation*

Despite the low amount of variations in protein carbonylation patterns after training, our analysis highlights a consistent number of spots carbonylated in both muscle types as emerges from the representative Oxyblots in Fig. 2. In particular, the ImageMaster 2D Platinum software detected 265±50 (control soleus muscle), 306±17 (trained soleus muscle), 191±31 (control tibialis anterior muscle) and 202±10 (trained tibialis anterior muscle) carbonylated spots. These data suggest the presence of a basal and supposedly physiological level of carbonylation (varying between rats, as indicate the standard deviation values) that slightly increases after training. In order to obtain a global pattern of carbonylation independently from physical activity and in order to minimize the biological variability between different individuals, the images of all Oxyblots were used to perform two synthetic gels (one for tibialis anterior and one for soleus) in which only spots present in at least 7 muscle samples (on a total of 8 muscles sample analyzed) were taken into account. This type of gel is obtained by averaging the positions, shapes and optical densities of the spots in a given set of gels [43,44]. Fig. 3 reports the synthetic gels obtained from soleus (A) and tibialis anterior (B) muscle Oxyblots. These synthetic gels represent the common carbonylation pattern that can be found in these two types of rat muscles. This pattern is independent both from training (in fact the oxidized spots were present both in untrained and trained muscles) and from biological variability between different individuals because the spots present in the synthetic gels were found carbonylated in at least 7 of 8 muscle samples. Comparisons between the two synthetic Oxyblots show that the global pattern of carbonylation varies between the two muscle types and partially reflects the different protein expression profile. The computer-aided analysis of the two synthetic Oxyblot carbonylation profiles pointed out a total of 148 spots in soleus and 122 in tibialis anterior.

3.6. *Identification of proteins carbonylated independently from training*

In order to identify carbonylated spots, we performed preparative gels which were then colloidal Coomassie-stained (Figs. 1s and 2s). The Oxyblot images were then matched to the corresponding colloidal Coomassie stained 2-DE gels and the spots that corresponded to carbonylated

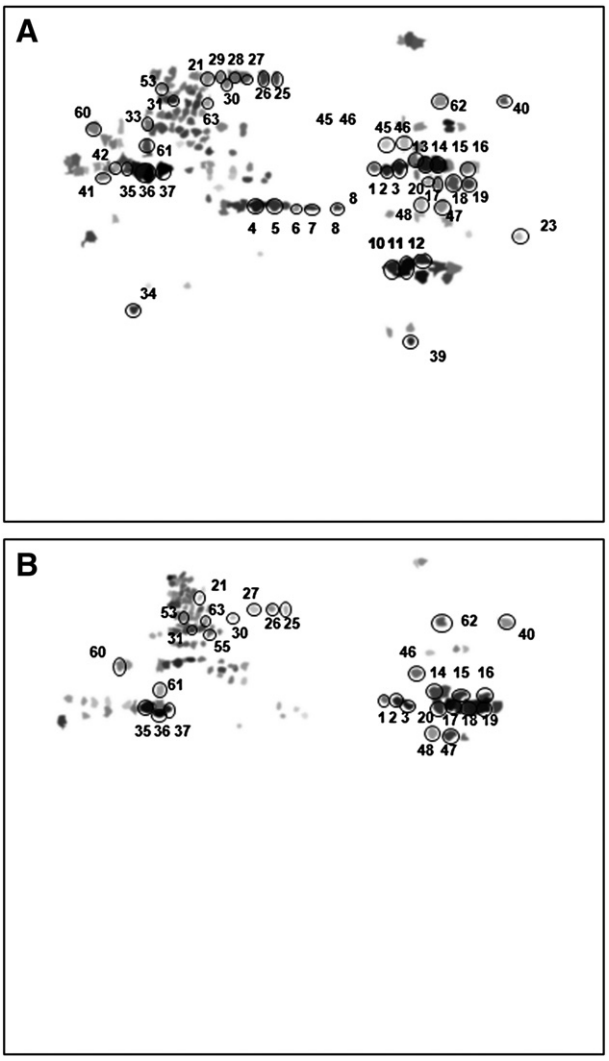

Fig. 3 – Synthetic gels representing the carbonylation pattern of soleus (panel A) and tibialis anterior (panel B) muscles. These gels were composed with the oxyblots images from all animals (untrained and trained) and show only the carbonylated spots matched in at least seven of the eight gels obtained from muscle samples. The spots identified by MS were indicated.

proteins were cut and subjected to mass spectrometry analysis. The increment of protein load caused an expected loss of separative power and some carbonylated spots, detectable with silver staining, were not clearly detected in Coomassie stained gels. Furthermore, analyzing Coomassie stained gels, we were unable to pick several carbonylated spots whose were clearly visible on Oxyblot acidic regions (Fig. 2), due to imprecise overlapping between two types of images (Oxyblot image and Coomassie stained gel image). We identified, by mass spectrometry, 30 protein spots in the tibialis anterior muscle and 47 in the soleus (Figs. 1s and 2s). Spots identified are indicated in Fig. 3 by circles and numbers. For detailed interpretation of our proteomic results, we categorized these proteins into five groups, according to functions. Category I includes proteins involved in anaerobic metabolism; category II consists of proteins involved in oxidative metabolism; category III covers structural proteins; category IV groups Hsp70 family chaperones and category V includes other proteins. The proteins belonging to these categories are reported in Table 4 and the mass spectrometry data of spots indicated in Table 4 and Fig. 3 are shown in Table 2s of supplementary materials.

3.6.1. *Category I: anaerobic metabolism*

Among the protein spots carbonylated in both types of muscle and involved in the carbohydrate metabolism we found several glycolytic enzymes: Glyceraldehyde-3-phosphate dehydrogenase (spots 47S, 47T, 48S and 48T), a key enzyme in glycolysis that catalyzes the first step of the pathway; 4 spots corresponding to Fructose-bisphosphate aldolase A (spots 17S, 17S, 18S, 18T, 19S, 19T, 20S and 20T) and Phosphoglycerate kinase 1 (spots 16S, 16T). We noticed that, while in soleus, which is predominantly characterized by aerobic metabolism, two Beta-enolase spots were carbonylated (spots 45S and 46S), in tibialis anterior only one is (spot 48T). A similar trend of carbonylation is shown by the mitochondrial Creatine kinase S-type; one spot was carbonylated only in soleus muscle (spot 13S) and three spots were carbonylated in both muscle types (spots 14S, 14T, 15S, 15T, 16S and 16T). On the other hand, three spots corresponding to the cytosolic isoform of Creatine kinase (M-type) were carbonylated both in soleus and in tibialis. As reported above, these proteins are involved in energy transduction in tissues with large energy demands.

3.6.2. *Category II: oxidative metabolism*

In category (II) we identified proteins involved in oxidative metabolism and in the respiratory chain. The cytoplasmic Malate dehydrogenase (spot 8S), resulted carbonylated only in soleus muscle. In this category we also found two mitochondrial proteins whose carbonylation is present in both muscles: a mitochondrial component of pyruvate dehydrogenase complex, the Dihydrolipoyllysine-residue acetyltransferase (spots 30S and 30T) that catalyzes the conversion of pyruvate to acetyl-CoA and CO_2 and subunits alpha and beta of mitochondrial ATP synthase (spots 40S, 40T, 60S and 60T). This complex produces ATP from ADP.

3.6.3. *Category III: structural proteins*

Many proteins belonging to this category are responsible for the generation of physical movement. Among these, we identified 4 spots of Troponin T (spots 4S, 5S, 6S and 7S). This protein resulted carbonylated only in soleus muscle, since it is typically expressed in slow-twitch fiber. We also identified: Myosin light chain 3, a regulatory light chain of myosin which does not bind calcium and was found to be carbonylated in the soleus (spot 34S) and Myosin-7, responsible for muscle contraction, carbonylated in both muscles (63S and 63T). This category also includes: two spots of Desmin, an intermediate filament found in muscle cells and carbonylated only in the Soleus muscle (spots 33S and 42S); and 4 spots of Alpha-actin, involved in cell motility and ubiquitously expressed in all eukaryotic cells (spots 35S, 35T, 36S, 36T, 37S, 37T, 61S and 61T). Finally we identified Testin (spots 55S and 55T) a scaffold protein involved in cell adhesion, cell spreading and in the reorganization of the actin cytoskeleton.

Table 4 – Identity of soleus and tibialis anterior muscle spots that appear carbonylated in all rats independently of training.

Spot no. [a]	Accession number [b]	Protein name
Anaerobic metabolism		
47S,47T	P04797	Glyceraldehyde-3-phosphate dehydrogenas
48S,48T	P04797	Glyceraldehyde-3-phosphate dehydrogenas
45S	P15429	Beta-enolase
46S,46T	P15429	Beta-enolase
17S,17T	P05065	Fructose-bisphosphate aldolase A
18S,18T	P05065	Fructose-bisphosphate aldolase A
19S,19T	P05065	Fructose-bisphosphate aldolase A
20S,20T	P05065	Fructose-bisphosphate aldolase A
16S,16T	P11617	Phosphoglycerate kinase 1
13S	P09605	Creatine kinase S-type, mitochondrial
14S,14T	P09605	Creatine kinase S-type, mitochondrial
15S,15T	P09605	Creatine kinase S-type, mitochondrial
16S,16T	P09605	Creatine kinase S-type, mitochondrial
1S,1T	P00564	Creatine kinase M-type
2S,2T	P00564	Creatine kinase M-type
3S,3T	P00564	Creatine kinase M-type
Oxidative metabolism		
8S	O88989	Malate dehydrogenase, cytoplasmic
30S,30T	P08461	Dihydrolipoyllysine-residue acetyltransferase component of pyruvate dehydrogenase complex, mitochondrial
40S,40T	P15999	ATP synthase subunit alpha, mitochondrial
60S,60T	P10719	ATP synthase subunit beta, mitochondrial
Structural proteins		
4S	Q7TNB2	Troponin T, slow skeletal muscle
5S	Q7TNB2	Troponin T, slow skeletal muscle
6S	Q7TNB2	Troponin T, slow skeletal muscle
7S	Q7TNB2	Troponin T, slow skeletal muscle
34S	P16409	Myosin light chain 3
63S,63T	P02564	Myosin-7
33S	P48675	Desmin
42S	P48675	Desmin
35S,35T	P68136	Actin, alpha skeletal muscle
36S,36T	P68136	Actin, alpha skeletal muscle
37S,37T	P68136	Actin, alpha skeletal muscle
61S,61T	P68136	Actin, alpha skeletal muscle
55T		Testin
Hsp70 family chaperones		
31S,31T	P63039	60 kDa heat shock protein, mitochondrial
53S,53T	P63018	Heat shock cognate 71 kDa protein
21S,21T	P48721	Stress-70 protein, mitochondrial
29S	Q07439	Heat shock 70 kDa protein 1A/1B
41S	P63018	Heat shock cognate 71 kDa protein
Others proteins		
23S	Q9Z2L0	Voltage-dependent anion-selective channel protein 1
25S,25T	P02770	Serum albumin
26S,26T	P02770	Serum albumin
27S,27T	P02770	Serum albumin
28S	P02770	Serum albumin
39S	P23982	Alpha-crystallin B chain
62S,62T	P14141	Carbonic anhydrase 3
10S	P14141	Carbonic anhydrase 3
11S	P14141	Carbonic anhydrase 3
12S	P14141	Carbonic anhydrase 3

3.6.4. *Category IV: Hsp70 family chaperones*

All proteins belonging to this category act as chaperones and cooperate in promoting the refolding and proper assembly of unfolded polypeptides generated under stress conditions. Members of this family resulted carbonylated in both the muscles types with the exception of the heat shock 70 kDa protein 1A/1B that was carbonylated exclusively in soleus (spot 29S). The identified proteins are: mitochondrial 60 kDa heat shock protein (spots 31S and 31T), the Heat shock 71 kDa (spots 53S and 53T) and the mitochondrial Stress-70 protein (spots 21S and 21T).

3.6.5. *Category V: other proteins*

Belonging to this category we found: voltage-dependent anion-selective channel protein 1, carbonylated only in the soleus muscle (spot 23S). This protein forms a channel through the mitochondrial outer membrane which allows the diffusion of small hydrophilic molecules. It may also participate in the formation of the pore complex that is responsible for the release of mitochondrial products that trigger apoptosis. We also identified Carbonic anhydrase 3, a major participant in liver response to oxidative stress, which is mainly carbonylated in the soleus with its five carbonylated spots (spots 10S, 11S, 12S, 39S and 62S) compared to its single carbonylated spot in tibialis (spot 62T). Finally we list in this category Serum albumin, (spots 25S, 26S, 27S, T27 and 28S) which results carbonylated in both muscle types.

3.7. *Validation of proteomic results*

In order to validate this proteomic result, the reduction of alpha and beta-enolase expression in tibialis anterior muscles after training was confirmed by Western blot analysis with specific antibodies as shown in Fig. 4, panel A. Twenty micrograms of proteins were loaded on 12% SDS-PAGE and transferred onto a PVDF membrane. For quantification, the intensities of the immunostained bands were normalized to the total protein intensity in the same blot, as measured by Coomassie brilliant blue. In Fig. 4, panel B, the histogram representing enolase expression variation, shows a reduction in enzyme expression.

In order to confirm that the identified proteins were electively carbonylated we chose two enzymes (aldolase A and enolase) and one structural protein (actin) to perform an immunoprecipitation/Oxyblot experiment. Fig. 4 panel C shows that all three immunoprecipitated proteins react with DNP-derivate antibodies.

3.8. *Determination of antioxidant enzymes activities and lipid peroxidation*

In order to evaluate the antioxidant mechanisms induced by training, we measured in both types of muscles and in both conditions (trained and untrained) the activity of two antioxidant enzymes: Catalase (CAT) and Superoxide Dismutase (SOD). Fig. 5

Notes to Table 4
[a] Spot numbers match those reported in the representative 2-DE images shown in Fig. 3.
[b] Accession number in Swiss-Prot/UniprotKB.

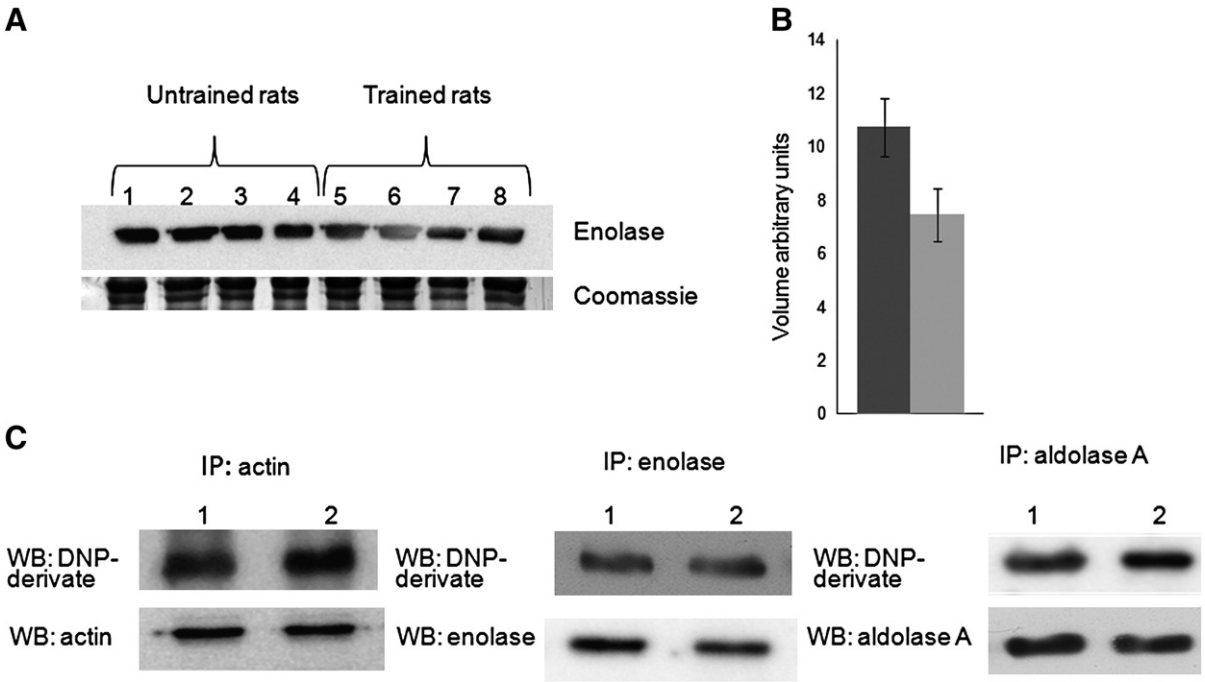

Fig. 4 – Validation of proteomic results. Panels A and B: enolase expression decrease induced by training. PVDF membrane was probed with antibodies against enolase isoforms identified by proteomic screening. Intensity of immunostained bands was normalized with the total protein intensities measured from the same blot stained with Coomassie brilliant blue (a representative band of the lane is reported); lanes 1, 2, 3 4 and lanes 5, 6, 7, 8 represent four untrained rats and four trained rats respectively. In panel B, histogram represents the average of enolase expression variation is reported. The two-tailed, non paired Student's t-test was performed. Panel C: immunoprecipitation/Oxyblot analysis. Actin, aldolase A and enolase were immunoprecipitated with respective antibodies and Western blot with anti-DNP antibodies was performed. The efficiency of immunoprecipitation was checked with the specific antibodies.

reports the Catalase (CAT) and Superoxide Dismutase (SOD) enzymatic activities, evaluated in both trained and untrained soleus and tibialis anterior muscles. CAT activity (panel A) decreased in both skeletal muscles in response to training ($p<0.01$). On the other hand, SOD-1 activity decreased (in tibialis anterior) or tended to decrease (in soleus) and SOD-2 increased (in soleus) or tended to increase (in tibialis anterior) in response to training. It should be stressed that the level of enzymatic activity may reflect the fact that the muscles had been subjected to recent exercise (the sacrifice occurred 1 h after the last training session). Moreover we observed no significant differences in lipid peroxidation after training, which were determined by measuring the malondialdehyde levels in both types of muscles (data not shown).

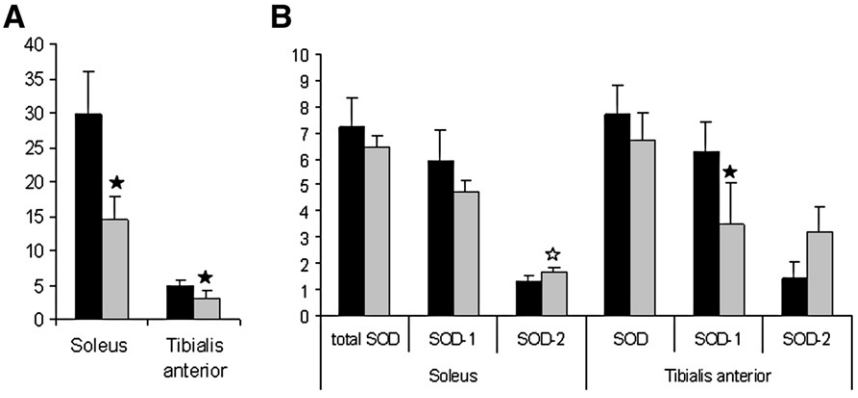

Fig. 5 – CAT (panel A) and SOD (panel B) activities in soleus and tibialis anterior muscles in untrained (black bars) and trained (gray bars) rats. Results are expressed as the mean ± SD of three independent measurements. Error bars indicate standard error. Black and white stars indicate SOD and CAT activities significantly different from control values ($p<0.01$ and $p<0.05$ respectively).

Table 5 – Muscles proteins found carbonylated in this and other papers independently from physical exercise or oxidative stress.

Protein name	Muscle type	References
Carbohydrate metabolism and TCA cycle		
Glyceraldhyde 3-phosphate dehydrogenase	Tibialis anterior [*] Soleus [*] Hind [45]	This work [*], Fedorova M. et al. J. Proteomics Res. 2010 [45]
Phosphoglycerate kinase 1	Soleus [*] Tibialis anterior [*]	This work [*]
Pyruvate kinase	Hind [45] Plantaris muscles [28]	Fedorova M. et al. J. Proteomics Res. 2010 [45] Burniston JG Biochim Biophys Acta. 2008 [28]
Fructose-bisphosphate aldolase	Soleus [*] Tibialis anterior [*] Hind [45] Gastrocnemious [46] Extensor digitorum longus (edl) [46]	This work [*] Fedorova M. et al. J. Proteomics Res. 2010 [45] Marin-Corral J et al. Antioxid Redox Signal. 2010 [46]
Dihydrolipoyllysine-residue acetyltransferase component of pyruvate dehydrogenase complex	Soleus [*] Tibialis anterior [*,45] Hind [45]	This work [*] Fedorova M. et al. J. Proteomics Res. 2010 [45]
Beta-enolase	Tibialis anterior [*] Soleus [*] Hind [45] Gastrocnemious [28] Edl [28]	This work [*] Fedorova M. et al. J. Proteomics Res. 2010 [45] Marin-Corral J et al. Antioxid Redox Signal. 2010 [3]
Dihydrolipoyllysine-residue succinyltransferase component of 2-oxoglutarate dehydrogenase complex	Hind [45]	Fedorova M. et al. J. Proteomics Res. 2010 [45]
Glycogen phosphorylase, muscle for	Hind [45]	Fedorova M. et al. J. Proteomics Res. 2010 [45]
Aldehyde dehydrogenase mitochondrial	Heart [46]	Marin-Corral J et al. Antioxid Redox Signal. 2010 [46]
Muscle contraction		
Troponin T, slow skeletal muscle	Soleus [*] Hind [45]	This work [*] Fedorova M. et al. J. Proteomics Res. 2010 [45]
Desmin	Soleus [*] Tibialis anterior [*] Hind [45]	This work [*] Fedorova M. et al. J. Proteomics Res. 2010 [45]
Myosin light chain 3, skeletal muscle isoform	Soleus [*] Tibialis anterior [*] Heart [46]	This work [*] Marin-Corral J et al. Antioxid Redox Signal. 2010 [46]
Myosin light chain 1, skeletal muscle isoform	Hind [45]	Fedorova M. et al. J. Proteomics Res. 2010 [45]
Myosin regulatory light chain 2, skeletal muscle isoform	Hind [45]	Fedorova M. et al. J. Proteomics Res. 2010 [45]
Actin, alpha skeletal muscle	Soleus [*,45] Tibialis anterior [*,45] Hind [45] Gastrocnemious [46] Edl [46] Heart [46]	This work [*] Fedorova M. et al. J. Proteomics Res. 2010 [45] Marin-Corral J et al. Antioxid Redox Signal. 2010 [46]
Tropomyosin	Hind [45] Gastrocnemious [46] Tibialis anterior [46] Heart [46] Soleus [46]	Fedorova M. et al. J. Proteomics Res. 2010 [45] Marin-Corral J et al. Antioxid Redox Signal. 2010 [46]
Myosin 6	Heart [46]	Marin-Corral J et al. Antioxid Redox Signal. 2010 [46]
Troponin T, fast skeletal muscle	Hind [45] Hind [45]	Fedorova M. et al. J. Proteomics Res. 2010 [45] Fedorova M. et al. J. Proteomics Res. 2010 [45]
Troponin I fast skeletal muscle	Hind [45]	Fedorova M. et al. J. Proteomics Res. 2010 [45]
Energy metabolism		
Creatine kinase M-type	Soleus [*,45] Tibialis anterior [*,45] Hind [45] Plantaris muscles [2] Gastrocnemious [46] Heart [46] Edl [46]	This work [*] Fedorova M. et al. J. Proteomics Res. 2010 [45] Burniston JG Biochim Biophys Acta. 2008 [28] Marin-Corral J et al. Antioxid Redox Signal. 2010 [46]

(continued on next page)

Table 5 *(continued)*

Protein name	Muscle type	References
Creatine kinase S-type	Soleus [*] Tibialis anterior [*]	This work [*]
ATP synthase subunit alpha	Soleus [*,] Anterior Tibial [*]	This work [*]
ATP synthase subunit beta	Hind, [45] Gastrocnemious [46] Heart [46] Soleus [46] Edl [46]	Fedorova M. et al. J. Proteomics Res. 2010 [45] Marin-Corral J et al. Antioxid Redox Signal. 2010 [46]
V-type proton ATPase subunit C	Heart [46]	J Marin-Corral J et al. Antioxid Redox Signal. 2010 [46]
NADH-ubiquinone oxidoreductase, 75 kDa subunit	Heart [46]	Marin-Corral J et al. Antioxid Redox Signal. 2010 [46]
Heath shock family		
Stress-70 protein mitochondrial	Soelus [*] Tibialis anterior [*]	This work [*]
Heat shock 70 kDa protein 1A/1B	Soelus [*] Tibialis anterior [*]	This work [*]
60 kDa heat shock protein, mitochondrial	Soelus [*] Tibialis anterior [*]	This work [*]
Heat shock cognate 71 kDa protein	Soleus [*]	This work [*]
78 kDa glucose-regulated protein	Hind [45]	Fedorova M. et al. J. Proteomics Res. 2010 [45]
Others		
Serum albumin	Soleus [*] Tibialis anterior [*] Plantaris muscle [28]	This work [*] Burniston JG Biochim Biophys Acta. 2008 [28]
Collagen α-1 chain	Hind [45]	Fedorova M. et al. J. Proteomics Res. 2010 [46]
Carbonic anhydrase 45	Soleus [*,45] Tibialis anterior [46] Hind leg muscle [45] Plantaris muscle [28] Gastrocnemious [46] Edl [46]	This work [*] Fedorova M. et al. J. Proteomics Res. 2010 [45] Burniston JG Biochim Biophys Acta. 2008 [28] Marin-Corral J et al. Antioxid Redox Signal. 2010 [46]
Voltage-dependent anion-selective channel protein	Soleus [*]	This work [*]

4. Discussion

It is well known that protein carbonylation depends on the presence of conjugated metals, on the position of specific amino acids in the protein structure, on the degree of oxidative stress in the compartment where the protein originated and on ROS concentration. The protein oxidation level and its variations following physical training have been investigated by many authors using a spectrophotometric assay of carbonyl content. While this method provides a global measurement of carbonylation it does not allow the identification of protein targets. In a previous paper we reported the characterization of plasma protein carbonylation in response to physical exercise in trained male endurance athletes, in order to obtain an overview of post-training plasma proteins oxidation [24].

In the present study, by using an experimental animal model, we analyzed the influence of aerobic training on protein expression and formation of carbonyl adducts in two types of rat skeletal muscle: tibialis anterior and soleus. As expected, we found that aerobic training induced a partial switch to aerobic metabolism in the tibialis anterior, basically a fast-twitch glycolitic muscle, where several proteins involved in glycolysis were downregulated. On the other hand, only few variations in protein expression profile were induced in soleus muscle (characterized by a mostly aerobic metabolism). Concerning protein carbonylation, the main objectives of this study were to explore whether oxidative modifications occur differentially in different types of skeletal muscle, both in terms of total amount of carbonylation and of fiber-type specificity of the proteins involved.

Proteomic analysis showed the presence of two categories of proteins: proteins endowed with a basal level of carbonylation independently of exercise and proteins whose carbonylation increased after training. About the former, our results underline the existence of a high basal level of protein carbonylation. Although this level shows some variation among individual animals, several protein spots appear carbonylated in all animals, in both types of skeletal muscle and independently of training. Most of these proteins are involved in energy metabolism, carbohydrate metabolism, muscle contraction and stress response. This indicates that many cellular proteins can be ROS targets regardless of their sequence and specific localization. Furthermore in soleus muscles the percentage of carbonylated proteins (number of spots present in WB/number of spots visible in silver stained gel) is higher than in tibialis anterior muscles (35% and 18% respectively), thus indicating that the aerobic metabolism promotes ROS formation and protein oxidation. It is worth underlining that the targets of

carbonylation are partially different between the two muscle types, mostly reflecting differences in protein expression patterns (see, for example, Troponin T and Carbonic anhydrase that are more expressed in soleus muscle than in tibialis anterior). Despite the differences observed in the two muscle types, this study brings to focus a basal level of carbonylation. Such basal level is common in mammalian tissues and it might to be due to the ability of proteins to act as ROS scavengers. Other recent publications [25] report basal levels of carbonylation in plasma and, in particular, in muscles [45,46] independently of exercise or oxidative stress (Table 5). An important challenge for future investigation in this field will be to understand the impact of carbonylation on specific proteins and to evaluate whether and in which circumstances this basal level, which is supposed well tolerated by cells, may increase as to hamper their functions. The latter group of carbonylated proteins includes those displaying a difference in oxidative damage between the trained and untrained muscles. Belong to this group Fructose-bisphosphate aldolase A and Carbonic anydrase 3 in soleus and Actin in tibialis anterior. Fructosebisphosphate aldolase A is a glycolytic enzyme that catalyzes the reversible aldol cleavage or condensation of fructose-1,6-bisphosphate into dihydroxyacetone-phosphate and glyceraldehyde 3-phosphate. Its catalytic mechanism is characterized by the formation of a Schiff base intermediate between a highly conserved active site lysine and a substrate carbonyl group. This feature is probably responsible of the fact that, together with many glycolytic enzymes, it is a common target of oxidation in aging tissues [47,48]. In turn, also Carbonic anydrase 3 was one of the first recognized targets of in vivo oxidative modification [49] in the aging process. Myofilament proteins such as Actin have been found to be particularly susceptible to oxidative damage; this topic has been extensively reviewed by Barreiro and Hussain [50], which flatly concluded that "… observations… suggest that …these modifications play important roles in regulating muscle function.". Moreover, two proteins belonging to the heat shock family were found to be more carbonylated in trained than in untrained conditions in both muscles. It has been shown that chaperons of the HSP70 family can physically interact with and prevent thermal inactivation of sarco(endo)plasmic reticulum Ca(2+)-ATPase (SERCA) 1a in skeletal muscle [51]. Since SERCA ATPases are easily inactivated by ROS [52], the possibility that molecular chaperons protect them from oxidation by taking on themselves the oxidative modifications is very enticing.

The increased carbonylation level may be correlated with the reduced CAT and SOD1 enzymes activity in both skeletal muscles. As reported by many authors, CAT expression decreases in muscles following physical activity [53,54]. It is still likely that the increase in the enzymatic activity of SOD-2 (the mitochondrial isoform of SOD) may reflect the need for an increased detoxification of ROS originating in the mitochondria as a consequence of the aerobic training. On the contrary the lipid peroxidation, measured by the malondialdehyde level, was unaffected, indicating no damage to skeletal muscle cell membranes after aerobic training. More studies will be necessary in order to understand the reason(s) for the differential carbonylation pattern in the two different muscle types and the selectivity of the oxidation targets.

Supplementary materials related to this article can be found online at doi:10.1016/j.jprot.2011.10.017.

Acknowledgment

This work was supported by the FIRB grant "Italian Human ProteomeNet" (BRN07BMCT_013),15 from Italian Ministry of University and Scientific Research to LB.

REFERENCES

[1] Reid MB. Nitric oxide, reactive oxygen species, and skeletal muscle contraction. Med Sci Sports Exerc 2001;33:371–6.
[2] Reid MB, Khawli FA, Moody MR. Reactive oxygen in skeletal muscle, III: contractility of unfatigued muscle. J Appl Physiol 1993;75:1081–7.
[3] Reid MB, Shoji T, Moody MR, Entman ML. Reactive oxygen in skeletal muscle, II: extracellular release of free radicals. J Appl Physiol 1992;73:1805–9.
[4] Powers SK, Talbert EE, Adhihetty PJ. Reactive oxygen and nitrogen species as intracellular signals in skeletal muscle. J Physiol 2011;589:2129–38.
[5] Mori H, Oikawa M, Tamagami T, Kumaki H, Nakaune R, Amano J, et al. Oxidized proteins in astrocytes generated in a hyperbaric atmosphere induce neuronal apoptosis. J Alzheimers Dis 2007;11:165–74.
[6] Brandes N, Schmitt S, Jakob U. Thiol-based redox switches in eukaryotic proteins. Antioxid Redox Signal 2009;11:997–1014.
[7] Jackson MJ. Redox regulation of skeletal muscle. IUBMB Life 2008;60:497–501.
[8] Magherini F, Carpentieri A, Amoresano A, Gamberi T, De Filippo C, Rizzetto L, et al. Cell Mol Life Sci 2009;66:933–47.
[9] Stadtman ER, Levine RL. Free radical-mediated oxidation of free amino acids and aminoacid residues in proteins. Amino Acids 2003;25:207–18.
[10] Mirzaei H, Regnier F. Protein:protein aggregation induced by protein oxidation. J Chromatogr B 2008;87:8–14.
[11] Chaudhuri AR, de Waal EM, Pierce A, Van Remmen H, Ward WF, Richardson A. Detection of protein carbonyls in aging liver tissue: a fluorescence-based proteomic approach. Mech Ageing Dev 2006;127:849–61.
[12] Goto S, Nakamura A, Radak Z, Nakamoto H, Takahashi R, Yasuda K, et al. Carbonylated proteins in aging and exercise: immunoblot approaches. Mech Ageing Dev 1999;107:245–53.
[13] Dalle-Donne I, Aldini G, Carini M, Colombo R, Rossi R, Milzani A. Protein carbonylation, cellular dysfunction, and disease progression. J Cell Mol Med 2006;10:389–406.
[14] Barreiro E, Hussain SN. Protein carbonylation in skeletal muscles: impact on function. Antioxid Redox Signal 2010;12:417–29.
[15] Wong CM, Cheema AK, Zhang L, Suzuki YJ. Protein carbonylation as a novel mechanism in redox signaling. Circ Res 2008;102:310–8.
[16] Wong CM, Marcocci L, Liu L, Suzuki YJ. Cell signaling by protein carbonylation and decarbonylation. Antioxid Redox Signal 2010;12:393–404.
[17] Agostini F, Dalla Libera L, Rittweger J, Mazzucco S, Jurdana M, Mekjavic IB, et al. Effects of inactivity on human muscle glutathione synthesis by a double-tracer and single-biopsy approach. J Physiol 2010;588:5089–104.
[18] Powers SK, Kavazis AN, McClung JM. Oxidative stress and disuse muscle atrophy. J Appl Physiol 2007;102:2389–97.

[19] Nuss JE, Amaning JK, Bailey CE, DeFord JH, Nuss JE, Amaning JK, et al. Oxidative modification and aggregation of creatine kinase from aged mouse skeletal muscle. Aging 2009;1: 557–72.
[20] Feng J, Xie H, Meany DL, Thompson LV, Arriaga EA, Griffin TJ. Quantitative proteomic profiling of muscle type-dependent and age-dependent protein carbonylation in rat skeletal muscle mitochondria. J Gerontol A Biol Sci Med Sci 2008;63: 1137–52.
[21] Silva LA, Pinho CA, Scarabelot KS, Fraga DB, Volpato AM, Boeck CR, et al. Physical exercise increases mitochondrial function and reduces oxidative damage in skeletal muscle. Eur J Appl Physiol 2009;105:861–7.
[22] Radák Z, Kaneko T, Tahara S, Nakamoto H, Ohno H, Sasvári M, et al. The effect of exercise training on oxidative damage of lipids, proteins, and DNA in rat skeletal muscle: evidence for beneficial outcomes. Free Radic Biol Med 1999;27:69–74.
[23] Fisher-Wellman K, Bloomer RJ. Acute exercise and oxidative stress: a 30 year history. Dyn Med 2009;8:1.
[24] Guidi F, Magherini F, Gamberi T, Bini L, Puglia M, Marzocchini R, et al. Plasma protein carbonylation and physical exercise. Mol Biosyst 2011;7:640–50.
[25] Madian AG, Regnier FE. Profiling carbonylated proteins in human plasma. J Proteome Res 2010;9:1330–43.
[26] Guelfi KJ, Casey TM, Giles JJ, Fournier PA, Arthur PG. A proteomic analysis of the acute effects of high-intensity exercise on skeletal muscle proteins in fasted rats. Clin Exp Pharmacol Physiol 2006;33:952.
[27] Boluyt MO, Brevick JL, Rogers DS, Randall MJ, Scalia AF, Li ZB. Changes in the rat heart proteome induced by exercise training: increased abundance of heat shock protein hsp20. Proteomics 2006;6:3154–69.
[28] Burniston JG. Changes in the rat skeletal muscle proteome induced by moderate-intensity endurance exercise. Biochim Biophys Acta 2008;1784:1077–86.
[29] Holloway KV, O'Gorman M, Woods P, Morton JP, Evans L, Cable NT, et al. Proteomic investigation of changes in human vastus lateralis muscle in response to interval-exercise training. Proteomics 2009;9:5155–74.
[30] Egan B, Dowling P, O'Connor PL, Henry M, Meleady P, Zierath JR, et al. 2-D DIGE analysis of the mitochondrial proteome from human skeletal muscle reveals time course-dependent remodelling in response to 14 consecutive days of endurance exercise training. Proteomics 2011;11:1413–28.
[31] Committee on Care and Use of Laboratory Animals. Guide for the care and use of laboratory animals. Bethesda: Natl. Inst Health; 1985 [DHHS Publ No (NIH)].
[32] Wessel D, Flügge A. Method for the quantitative recovery of protein in dilute solution in the presence of detergents and lipids. Anal Biochem 1984;138:141–3.
[33] Hochstrasser DF, Patchornik A, Merril CR. Development of polyacrylamide gels that improve the separation of proteins and their detection by silver staining. Anal Biochem 1988;173: 412–23.
[34] Neuhoff V, Arold N, Taube D, Ehrhardt W. Improved staining of proteins in polyacrylamide gels including isoelectric focusing gels with clear background at nanogram sensitivity using Coomassie Brilliant Blue G-250 and R-250. Electrophoresis 1988;9:255–62.
[35] Dalle-Donne I, Rossi R, Giustarini D, Gagliano N, Di Simplicio P, Colombo R, et al. Methionine oxidation as a major cause of the functional impairment of oxidized actin. Free Radic Biol Med 2002;32:927–37.
[36] Hellman U, Wernstedt C, Gonez J, Heldin CH. Improvement of an "in gel" digestion procedure for the micropreparation of internal protein fragments for amino acid sequencing. Anal Biochem 1995;224:451–5.
[37] Góth LA. Simple method for determination of serum catalase activity and revision of reference range. Clin Chim Acta 1991;196:143–51.
[38] Abruzzo PM, di Tullio S, Marchionni C, Belia S, Fanó G, Zampieri S, et al. Oxidative stress in the denervated muscle. Free Radic Res 2010;44:563–76.
[39] Peskin AV, Winterbourn CC. A microtiter plate assay for superoxide dismutase using a water-soluble tetrazolium salt (WST-1). Clin Chim Acta 2000;293:157–66.
[40] Ohkawa H, Ohishi N, Yagi K. Assay for lipid peroxides in animal tissues by thiobarbituric acid reaction. Anal Biochem 1979;95:351–8.
[41] Pancholi V. Multifunctional alpha-enolase: its role in diseases. Cell Mol Life Sci 2001;58:902–20.
[42] Lopez-Alemany R, Suelves M, Diaz-Ramos A, Vidal B, Munoz-Canoves P. Alpha-enolase plasminogen receptor in myogenesis. Front Biosci 2005;10:30–6.
[43] Terzuoli L, Felici C, Ciari I, Guerranti R, Pagani R, Marinello E, et al. Synthetic gel of carotid artery plaque. Int J Immunopathol Pharmacol 2007;20:637–42.
[44] Luhn S, Berth M, Hecker M, Bernhardt J. Using standard positions and image fusion to create proteome maps from collections of two-dimensional gel electrophoresis images. Proteomics 2003;7:1117–27.
[45] Fedorova M, Kuleva N, Hoffmann RJ. Identification, quantification, and functional aspects of skeletal muscle protein-carbonylation in vivo during acute oxidative stress. Proteome Res 2010;9:2516–26.
[46] Marin-Corral J, Fontes CC, Pascual-Guardia S, Sanchez F, Olivan M, Argilés JM, et al. Redox balance and carbonylated proteins in limb and heart muscles of cachectic rats. Antioxid Redox Signal 2010;12:365–80.
[47] Martínez A, Dalfó E, Muntané G, Ferrer I. Glycolitic enzymes are targets of oxidation in aged human frontal cortex and oxidative damage of these proteins is increased in progressive supranuclear palsy. J Neural Transm 2008;115:59–66.
[48] Gómez A, Ferrer I. Increased oxidation of certain glycolysis and energy metabolism enzymes in the frontal cortex in Lewy body diseases. J Neurosci Res 2009;87:1002–13.
[49] Cabiscol E, Levine RL. Carbonic anhydrase III. Oxidative modification in vivo and loss of phosphatase activity during aging. J Biol Chem 1995;270:14742–7.
[50] Barreiro E, Hussain SN. Protein carbonylation in skeletal muscles: impact on function. Antioxid Redox Signal 2010;12: 417–29.
[51] Fu MH, Tupling AR. Protective effects of Hsp70 on the structure and function of SERCA2a expressed in HEK-293 cells during heat stress. Am J Physiol Heart Circ Physiol 2009;296: H1175–83.
[52] Sun J, Xu L, Eu JP, Stamler JS, Meissner G. Classes of thiols that influence the activity of the skeletal muscle calcium release channel. J Biol Chem 2001;13:15625–30.
53 Laughling MH, Simpson T, Sexton WL, Brown OR, Smith JK, Korthuis RJ. Skeletal muscle oxidative capacity, antioxidant enzymes, exercise training. J Appl Physiol 1990;68:2337–43.
[54] Powers SK, Criswell D, Lawler J, Ji LL, Martin D, Herb RA, et al. Influence of exercise and fiber type on antioxidant enzyme activity in rat skeletal muscle. Am J Physiol Regul Integr Comp Physiol 1994;266:R375–80.